KaRIn: Ka-band Radar Interferometer On-Board Processor (OBP) for Land Algorithm Theoretical Basis Document (ATBD)

JPL Document: D-55533

Revision B

Nov 08, 2017

National Aeronautics and Space Administration
Jet Propulsion Laboratory
California Institute of Technology

KaRIn: Ka-band Radar Interferometer On-Board Processor (OBP) for Land Algorithm Theoretical Basis Document (ATBD)

PREPARED BY (CUSTODIAN):

Electronic signature on file — *12/13/2017*

Samuel Chan / KaRIn Performance Engineer — Date

APPROVED BY:

Electronic signature on file — *11/13/2017*

Daniel Esteban-Fernandez / KaRIn Instrument Manager — Date

Electronic signature on file — *12/1/2017*

Lee-Leung Fu / SWOT Project Scientist — Date

Electronic signature on file — *11/13/2017*

Eva Peral / KaRIn System Engineer — Date

Electronic signature on file — *12/12/2017*

Daniel Limonadi / Payload System Engineer — Date

Electronic Signatures in PDMS

D-55533, B : KARIN ON-BOARD PROCESSOR (OBP) FOR LAND, ALGORITHM THEORETICAL BASIS DOCUMENT (ATBD)

Work Description	Signature Stamp	Time In	Signed off By	Signed off Date	Comments
Release Authority - Attach files and check format. Please verify correct metadata before releasing	None	12/13/2017 8:59:01 AM	$GRP		
Approver - Approve Document for Release	Approved - Standard	11/13/2017 10:23:38 AM	SAMUEL F CHAN (schan)	12/13/2017 8:58:58 AM	
Approver - Approve Document for Release	Approved - Standard	11/13/2017 10:23:37 AM	LEE-LUENG FU (llf)	12/1/2017 2:51:15 PM	
Approver - Approve Document for Release	Approved - Standard	11/13/2017 10:23:37 AM	EVA PERAL (eperal)	11/13/2017 8:04:20 PM	
Approver - Approve Document for Release	Approved - Standard	11/13/2017 10:23:37 AM	DANIEL LIMONADI (dlimo)	12/12/2017 10:52:33 AM	change log file references do not match the file names that are in PDMS for initial and rev A versions of the document. Not holding up signature for this, but should be fixed in next revision.
Approver - Approve Document for Release	Approved - Standard	11/13/2017 10:23:37 AM	DANIEL ESTEBAN-FERNANDEZ (dani)	11/13/2017 11:45:55 AM	
Submitter Signature		11/13/2017 10:23:35 AM	JOSHUA C HEIN (hein)		

Change Number	Change Date	Changes / Notes
JPL_KaRIn_OBP_land_ATBD_v0.docx	Sept. 14, 2015	Initial Release
JPL_KaRIn_OBP_land_ATBD_initial.docx	June 30, 2016	Requirements are updated according its latest version – section 2, p.7 The order of presumming and range filtering/subsampling is reversed in the processing – section 3, p.9 The filter for range filtering/subsampling is changed from the combination of Parks-McClellan filter and sinc interpolation filter to Third-band Nyquist filter – section 4.2 and 5.2, p.13-14 and p.18-23 In Doppler removal, phase shift of last line in previous DC block is added to the phase ramp of current block to maintain phase continuity between blocks – section 4.1, p.12 Analysis results in evaluating performance are presented – section 5.1 and 5.4, p.15-18, p.23-24 Calibration scheme, processing boundaries and downlinked data are summarized – section 4 and Appendix B, p.9-12 and p.28 Expanded sections 1, 2.1, 3, and 4.3.
JPL_KaRIn_OBP_land_ATBD_RevB_20171108	Nov 08, 2017	Rev B: Fixed land DWL, p.8 Doppler centroid estimation is constant across swath. Add option of Doppler removal with ground predicted Doppler centroid p.8, 9, 14, 15 Update summary of calibration, p.12 For proper presumming - land data buffer for DWP change and DWP shift for aligning chirp center as pulse width change, p. 16, 17, 25

Table of Contents

List of Acronyms

AASR	Azimuth Ambiguity to Signal Ratio
BW	Chirp bandwidth
DORIS	Doppler Orbitography and Radio positioning Integrated by Satellite
ECCO2	Estimating the Circulation and Climate of the Ocean, Phase II
HW	Hardware
ISLR	Integrated Sidelobe Ratio
KaRIn	Ka-band SAR interferometric radar
MLE	Maximum Likelihood Estimator
MSS	Mean Sea Surface
NB	Number of beams produced during azimuth compression
NP	Number of pulses used for azimuth compression
OBP	On-Board Processor
PBW	Processing Bandwidth
RMS	Root Mean Square
SADC	Science Analog to Digital Converter
SAR	Synthetic Aperture Radar
S/C	Spacecraft
SLA	Sea Level Anomaly
SWOT	Surface Water and Ocean Topography
WGS84	World Geodetic System 1984

1 Introduction

The Surface Water and Ocean Topography (SWOT) mission is a partnership between two communities, physical oceanography and hydrology, to share high vertical accuracy topography data produced by the payload, whose principal instrument is the Ka-band Radar Interferometer (KaRIn). The details of SWOT mission objectives and requirements can be found in the SWOT Science Requirements Document [1]. The broad scientific goals can be summarized as follows:

Oceanography: characterize the ocean mesoscale and submesoscale circulation determined from the ocean surface topography at spatial resolutions of 15 km (for 68% of the ocean).

Hydrology: To provide a global inventory of all terrestrial surface water bodies whose surface area exceeds $(250m)^2$ (goal: $(100m)^2$, threshold: $1km^2$) (lakes, reservoirs, wetlands) and rivers whose width exceeds 100m (goal: 50m, threshold: 170m). To measure the global storage change in terrestrial surface water bodies at sub-monthly, seasonal, and annual time scales. To estimate the global change in river discharge at sub-monthly, seasonal, and annual time scales.

This document describes the SWOT On-board processing (OBP) for hydrology. The intent of this algorithm is to provide the data necessary to meet the surface-water science requirements, for which high spatial resolution is necessary to discriminate between land and water, while undergoing minimal processing on-board in order to reduce the data rate to fit flight and ground downlink constraints. Such processing involves filtering and decimating, and reduction of the bit depth of each sample, to achieve a reduction factor of approximately 17 times lower data rate than that of the raw digital samples (349 Mbps vs. 6 Gbps). The compressed data are downlinked to the ground, where further processing will be performed to generate interferograms and height data. The ground processing of land data is not discussed in this document.

While nominally the on-board algorithm performs these processing steps all the time, actual downlink of the high-resolution data is controlled autonomously through the use of the so-called high-resolution mask stored on board. The high-resolution mask can be updated on a seasonal basis. The extent of the Earth surface area that can be covered by the high-resolution mask is constrained by the onboard storage capacity of the spacecraft Solid State Recorder, power constraints related to the X-Band Telecom system, and data rate and volume considerations throughout the ground system.

2 On-Board Processor for Land Key Requirements

The OBP requirements trace to the **SWOT Science Requirements Document** (JPL D-61923), shown below for reference, via the KaRIn Instrument Functional and Performance requirements.

2.4.1 [Requirement] The Baseline Science Mission shall operate for at least 42 months, including three annual cycles (36 months), a 3-month phase of launch/early operation and payload check out, and a 3-month fast-sampling calibration phase (including orbit transition).

2.6.3.a [Requirement] The following Level-2 standard data products shall be produced for the surface water data:

- For each pass, a geolocated water mask of all water bodies identified in the data downlinked by SWOT, regardless of surface area. The mask resolution will be reported at the finest resolution consistent with meeting appropriate geolocation accuracy. The mask will be reported as a geolocated point cloud (including data described below), which will have irregular spatial sampling and varying average point separation from near to far range.
- SWOT required performance will be evaluated using water bodies meeting the minimum size criteria set in the science requirements, i.e., water bodies with area greater than (250 m)^2 and rivers of width greater than 100 m However, the SWOT performance will be characterized for water bodies meeting the minimum size criteria in the science goals; i.e., water bodies with area greater than (100 m)^2 and rivers of width greater than 50 m. Only water bodies in regions of moderate topographic relief (i.e., where layover contamination is negligible) are to be used to assess SWOT performance.
- Estimated surface water elevations with the same sampling as the water mask.
- Estimated surface water elevation uncertainties (1σ) with the same sampling as the water mask.
- Estimated surface area represented by each point in the pixel cloud with the same sampling as the water mask.
- Additional data and meta-data (e.g., collection time, water brightness) that might be required for deriving additional data products.

2.8.2.a [Requirement] The surface water areas estimated using the Level-2 water mask shall have a relative error smaller than 15% (1σ) of the total water body area for water bodies whose non-vegetated surface area exceeds (250m)^2 or river reaches whose width exceeds 100 m on average and length exceeds 10 km.

2.8.3 [Requirement] The lake and reservoir, height accuracy of the Level-2 data shall be (1) 10 cm (1σ) or better, for water bodies whose non-vegetated surface area exceeds 1 km^2 and (2) 25 cm or better for water bodies whose non-vegetated surface area is between (250m)^2 and 1 km^2.

2.8.5 [Requirement] Using the Level-2 data, after processing elevations over a maximum 10 km of flow distance, river water slope accuracy shall be 1.7 cm/1km (17 µrad) (1σ) or better for river widths greater than 100 m.

2.1 OBP for Land Functional Requirements

- *Input*
  - The OBP shall interface and receive two I/Q echoes (one from each channel) in real-time from the Science ADCs (SADCs).
  - The OBP shall receive processing parameters from flight software (FSW).
- *Processing*
  - The OBP shall process a fixed number of samples (or fixed data window length, DWL) for all PRFs.
  - The OBP shall perform Doppler centroid estimation from sADC raw data.
  - The OBP shall remove Doppler centroid from raw data. It shall use the on-board estimation of the Doppler centroid plus a Doppler centroid correction that is stored in a canned table, or bypass the on-board estimation and use a predicted Doppler that is stored in a canned table. The tables can be re-uploaded from the ground.
  - The OBP shall filter and subsample data in range direction with a fixed output sampling rate of 200 MHz.
  - The OBP shall presum data in azimuth direction with a set of filter coefficients stored in an on-board table and distributed by FSW. The set of filter coefficients is selected by a parameter in the parameter table of FSW. This parameter can be updated if a new presumming factor should be used.
  - The OBP shall compress rangeline data with Block Floating Point Quantization (BFPQ) [2].
- *Product generation*

A list of the information downlinked is described in Appendix B. At a high level, the key outputs that will be produced by the land algorithm and downlinked to the ground are:

- The estimated Doppler centroid
- The BFPQ compressed data from both interferometric channels for each swath

2.2 OBP for Land Operating Requirements

- The OBP shall accept commands and triggers from the CTU to process the incoming data.
- The OBP shall accept processing parameters from the FSW to process the incoming data.

3 Algorithm Description Overview

This section provides a high level overview of the OBP algorithm for land (a description in pseudo-code can be found in Appendix A).

The block diagram of the OBP algorithm for land is illustrated in Figure 1. The two received echoes (one from each channel) in I/Q format from the SADC board are processed independently. The processing steps are as follows:

1. Doppler removal
    a. Through a parameter in the static parameter table[1], the OBP can be controlled to perform the Doppler centroid removal with either the estimated Doppler centroid plus the Doppler centroid correction that is stored in a canned table (option 1) or the predicted Doppler centroid stored in a canned table (option 2).
    b. Option 1: Doppler centroid removal with the estimated Doppler centroid
        i. Doppler centroid is estimated by averaging phase differences between adjacent rangelines
        ii. The data is averaged in range in two range windows (see ocean ATBD [3]). The land Doppler centroid is computed as a weighted average of these two windows, resulting in a constant value across the swath.
        iii. The OBP adds the Doppler centroid correction that is stored in a canned table to the estimated Doppler frequency to form the corrected Doppler centroid.
    c. Option 2: Doppler centroid removal with the predicted Doppler centroid
        i. The OBP bypasses the on-board estimation and uses the predicted Doppler centroid, which is stored in a canned table, as the Doppler centroid
    d. With the Doppler centroid estimation from either option, azimuth phase ramps are generated and applied to the data to remove the Doppler prior to range filtering and subsampling[2].
2. Filtering and resampling data in the range direction
    a. Filtering is applied to remove excess bandwidth and interpolating data for resampling
    b. Rangeline data are run through this filter, and the sampling rate is reduced from 300 MHz to 200 MHz.
3. Presumming data in the along track direction

[1] Static parameter table is one of FSW uplink tables.
[2] Note that the Doppler removed in the OBP should be added back as part of the ground processing.

a. The presumming filter coefficients are received from FSW. There are two possible sets and they are corresponding to the presumming factor 2.125 or 2.4375. The baseline is 2.125.

4. Performing BFPQ of rangeline data.

   a. Data will be compressed with BFPQ, going from the data bitwidth at the output of the presumming block to 3-bits mantissa and 5-bits exponent with block size 32 and transferring to the onboard storage.

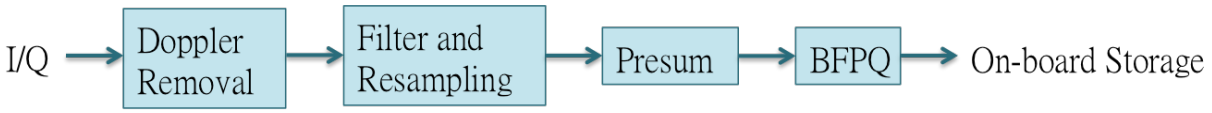

Figure 1. Block diagram of On-Board Processor for land

Note that, while the algorithm performs these processing steps all the time, the actual land data that goes out to the on-board storage is controlled by the downlink mask, an on-board table that defines the times in the orbital cycle (which map into actual regions of the orbit's coverage) where the data is outputted to the SSR for downlink. During nominal science operations, new the downlink masks can be uplinked to KaRIn on a seasonal basis, if desired, in order to cover different portions of Earth with land-processed data (within the coverage provided by the orbit trajectory).

4 Description of Algorithm

This section provides some details of the processing algorithm steps for SWOT land data. In Figure 2, the SWOT mission measurement concept is illustrated.

The KaRIn measurement data covers two swaths, located from 10 to 60 km on each side of the nadir track. They are called the left and right swaths according to their looking directions relative to the flight direction. There are two antennas at the ends of the baseline and they are called the left or right antennas depending on which swath they are closest to. For each swath, echoes will be received from both left and right antennas; hereafter referred to as left and right channels for a given swath. These terminologies will be used in the following algorithm description.

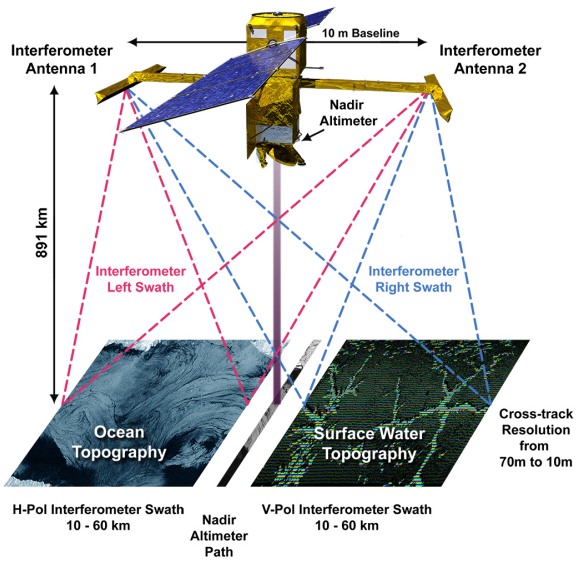

Figure 2. Conceptual illustration of the SWOT mission measurement concept. The Ka-band Radar Interferometer (KaRIn) illuminates two swaths of 50 km (±10 to 60 km on each side of the nadir track)

The thermal environment of KaRIn will vary over the course of the mission, potentially affecting the characteristics of the radar's signal path. To achieve the high accuracy requirement imposed on KaRIn, these characteristics are captured in order to perform SAR processing with the correct set of parameters. In particular, a calibration scheme is designed to obtain a replica of the transmit signal with high fidelity (which is used in the range compression stage of the ocean processing). While the calibration scheme is not applied on-board for the land processing, the information is downlinked to the ground with the intention that ground processing will (or has the option to) use it. Therefore, a summary of the calibration approach is discussed hereafter so as to provide the necessary information for the ground algorithms to apply any necessary corrections.

The electronic design for the calibration is shown in Figure 3. There are three calibration paths, and they are transmit loopback (TxLB), receiver calibration (RxCal) and hyberbox calibration (HB).

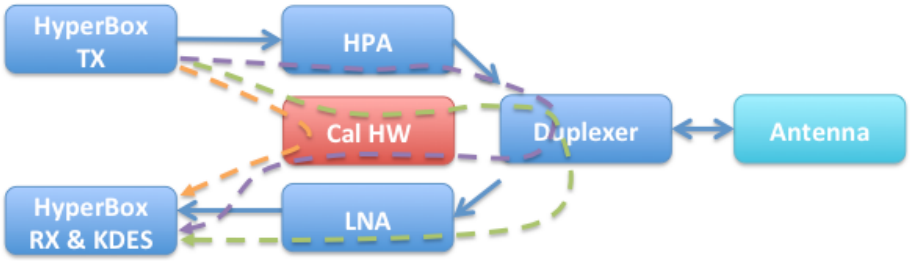

Figure 3. KaRIn calibration paths: transmit loopback (purple), receiver calibration (green) and hyberbox calibration (orange).

The signals from the three calibration paths will be averaged in the time domain over a specified time interval. The details about the calibration scheme can be found in the ocean ATBD [3]. The calibration data, transmit loopback, receiver calibration and hyperbox calibration, are stored in the calibration frames and they are downlinked to the ground. The ground processing for the surface water measurements has the option to use these calibration data to perform SAR processing and/or ground corrections.

As KaRIn goes along its orbit, some radar parameters need to be adjusted in order to receive the echoes from the desired swaths. For example, the pulse repetition frequency (PRF) changes as the slant range from the radar to the center of the swath varies because of the ellipsoidal shape of the Earth. These changes impose some processing boundaries in the OBP, like PRF change in this case. In addition, the OBP for ocean implements squinted unfocused azimuth SAR processing; this processing chain operates on the basis of dividing data into blocks at different levels, dictating several type of time scales (boundaries) that are relevant for the land processing. The relevant boundaries for the OBP for land are:

- Aperture Length (AL): the time internal corresponding to 9 PRIs, and they are pulses used in the squinted unfocused azimuth SAR processing
- Azimuth Pixel Posting Boundary (PB): 162 PRIs, which is the number of PRIs between azimuth ocean pixels after averaging. In terms of ground along-track distance, it corresponds to 250 m.
- Azimuth Pixel Length Boundary (PL): 648 PRIs, which is the number of PRIs used to compute one ocean pixel.
- Calibration Averaging Boundary (AV): 3,240 PRIs, which is the number of PRIs between calibration averaging intervals. Note that this boundary is offset by PB/2 from PB boundary.
- Doppler centroid estimation boundary for ocean (DL_ocean) and land (DL_land): both of them are AV * N PRIs, where N is an integer. The length for land shall be an integer multiple of the ocean one. Also, land and ocean boundaries shall be aligned with the same AV boundaries.

The lengths of these boundaries and their offsets are shown in Figure 5 and 6. Some important considerations of these boundaries for the OBP of land are noted. PRF changes are applied on AV boundaries. As DL_land is an integer multiple of AV, the minimum number of rangelines to estimate Doppler centroid for land is 3,240, and the nominal value is 32,400, to provide the required accuracy of Doppler centroid.

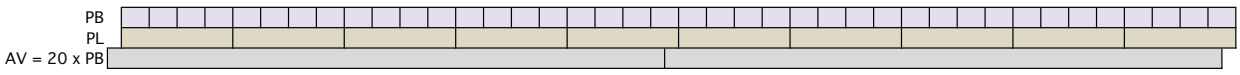

Figure 5. Lengths and offsets of boundaries PB, PL and AV.

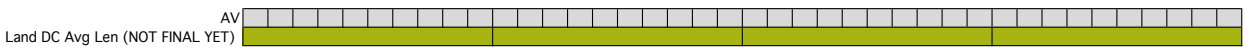

Figure 6. Length and offset of DL_land. It shows a nominal value of AV*10.

4.1 Removing Doppler

The azimuth sampling rate, or PRF, limits the highest observable Doppler frequency; only frequencies between -0.5PRF and +0.5PRF can be observed. The Doppler frequency component in this range is referred to as the fractional Doppler centroid. There are two possible options for the OBP to obtain the fractional Doppler centroid. It can be either estimated from the raw science data or predicted from the ground and sent through FSW table. A description for each option is given in the following.

Option 1: Doppler removal with estimating Doppler centroid

The fractional Doppler centroid is estimated by the phase differences between consecutive rangelines in a block of data, named Doppler centroid estimation block and its length being DL_land. The phase differences are evaluated and averaged in both range and azimuth directions using rectangular windows, and the averaging intervals are specified in tables. The averaged data are used in a weighted linear fit, and the weights are selected to get the Doppler centroid to be constant across the swath. This approach provides better performance for low sigma0's than the linear fit over a reference ground range that is used for ocean processing.

For each swath, there are two channels corresponding to the received echoes from the left and right antennas. The Doppler centroid is estimated for each channel independently. From these two estimates, their mean is actually the value used during the Doppler removal step. Since the left and right swaths produce separate (and generally different) mean Doppler centroid estimates, there is a total of six Doppler centroid estimations (two channels and their mean for each swath), which are incorporated in the calibration frame, and downlinked to the ground. A summary of the key data downlinked is provided in Appendix B.

Note that the calculated Doppler centroid from a data block is actually applied to the next data block. Thus, there is a time difference between the Doppler centroid being estimated and being applied; a correction for the known Doppler centroid shift corresponding to this temporal separation is computed by FSW from the information in the Doppler centroid correction table[3]. This correction will be calculated every AV. The OBP receives the Doppler correction and generates the corrected Doppler centroid.

To remove the Doppler frequency, a phase ramp is formed and applied in the azimuth direction for each range bin with the corrected Doppler centroid. The continuity of phases in the azimuth direction is ensured by storing the phases (as a function of cross track) applied to the last azimuth line of the previous Doppler centroid estimation block, and added to the phase ramps of the current block. The FSW-computed Doppler centroid correction and the phases applied to the last azimuth line of a data block are also downlinked to the ground as part of the calibration frame.

Option 2: Doppler removal with ground predicted Doppler centroid

[3] Doppler centroid correction table is one of FSW uplink table.

In general, the science data over land have lower signal-to-noise ratio than ocean as the sigma0 of land. The land Doppler estimation block size can be increased to improve the accuracy of the Doppler centroid estimate. However, the potential large scene contrast and the topography may still degrade the accuracy of the estimated Doppler centroid. In addition, studies indicate that the S/C attitude and KaRIn pointing is fairly stable. In that case, the Doppler centroid might be predicted on the ground with a higher dregree of accuracy than the on board estimation.

In this option, the FSW Doppler correction table will be populated with the ground predicted Doppler centroid. At every AV, the Doppler centroid is evaluated and passed to the OBP. Through a parameter in the static parameter table, it will control the OBP to take the FSW delivered "Doppler correction" as the exact Doppler centroid (ignore the estimated Doppler centroid). With this Doppler, the phase ramp is generated and the steps after it are the same as option 1.

4.2 Filtering and resampling data in the range direction

The transmit chirp pulse width changes with PRF in order to maintain a constant duty cycle of HPA. As the chirp rate is constant, the chirp bandwidth increases with its pulse width. The maximum transmit bandwidth can in theory be up to 210 MHz; however, the output sampling rate of data over land is fixed at 200 MHz, and therefore any excess chirp bandwidth will be filtered out to avoid aliasing. A Third-Band Nyquist filter is designed to perform both filtering the excess bandwidth and interpolating the data in a single step. The input sampling rate to the land processor is 300 MHz, and the data is subsampled by a factor of 2/3 with the output rate 200 MHz.

This step of processing requires a downsampling factor of 3. A third-band Nyquist filter is computational efficient for this configuration. It has the property that one-third of the coefficients are zero, and it is symmetric about the center coefficient. By taking advantage of the zero coefficients, the number of multiplications and additions for a third-band Nyquist filter can be reduced by about one-third of a symmetric finite-duration impulse-response filter of the same length. In addition, with the current FPGA technology, the data lines and the DSP blocks can be designed to achieve high speed processing with a reasonable amount of resources for this filter.

A third-band Nyquist filter can be designed using the windowed-sinc method, with coefficients given by equation below.

$$h[n] = \frac{1}{3} w[n] \operatorname{sinc}\left(\frac{n}{3}\right) \tag{1}$$

Window function $w[n]$ can be any window type, and Hamming being chosen for the current design. The range of n is from –(N-1)/2 to (N-1)/2, with N being the number of coefficients, which should be odd.

From $h[n]$, two filters are generated with downsampling-by-2, and they are named the even and the odd filters and their names are based on the coefficient indices. The even filter has an odd number of

coefficients and is symmetric about the center of the filter, i.e., symmetric about the zeroth coefficient. The odd filter has an even number of coefficients, and is symmetric about the center of the filter. Both of these filters can exploit symmetry to reduce the number of operations required to implement them. The third-band Nyquist filter with N = 31 is shown in Figure 7. The even and odd filters are shown in blue and red color respectively.

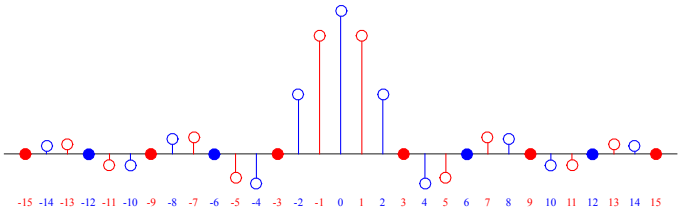

Figure 7: Third-Band Nyquist filter coefficients for length 31. (Blue is even filter and red is odd filter)

The delay of a digital filter with N coefficients is (N-1)/2. The even filter has an odd number of coefficients, so it calculates output samples at a whole sample delay relative to the input samples. The odd filter has an even number of coefficients, so it calculates output samples at a half-sample delay relative to the input samples.

After the raw data from SADC have undergone the Doppler removal step, they are injected into range filtering. When data with sampling rate 300 MHz go through these two filters, data with whole sample delay and half-sample delay are generated. This filtered data is subsampled-by-3 to form the desire output with sampling rate 200 MHz.

4.3 Presumming Data in the along track direction

To reduce the data rate and volume, the range filtered and subsampled data is presummed in azimuth. Presumming is equivalent to filtering and subsampling in azimuth. This is implemented with a filter bank that allows to implement presumming (i.e. decimation) factors that are multiples of 0.0625. The filter window is designed to remove excess bandwidth and avoid aliasing. Two presumming factors are supported by SWOT which can be selected during flight, either 2.125 or 2.4375. The current baseline value of the presumming factor is 2.125.

The change of the topography will lead to the change of the data window position (DWP), which controls the beginning of data collection within a pulse. (In the current design, the change of DWP can be either plus or minus 48 samples at 300 MHz sampling rate every 36 PRIs.) To allow proper presumming to be done across the boundary of DWP change, there is always a buffer or 48 samples at both ends of each rangeline. It guarantees all presum data are valid.

The pulse width of the transmit chirp might change associated with PRF change as mentioned in section 4.2. The data collected with different pulse widths across the PRF change boundary needs to have their

centers of the chirps (instead of their beginning) aligned in order to do the presumming appropriately. This is achieved by introducing an offset in DWP, which corresponds to half of the difference of pulse widths.

4.4 Performing BFPQ of rangeline data

To meet the allocated output data rate 349 Mbps, rangeline data is compressed with Block Floating Point Quantization (BFPQ). Therefore, the data will go from their bitwidth at the output of the presumming block to a 3-bits mantissa and 5-bits exponent, with block size 32 complex samples. The number of samples collected in a rangeline will be selected such that there are an integral number of BFPQ blocks after range filtering and resampling.

5 Performance

The processing steps of land data will introduce some systematic and random errors. The performance of each step of the algorithm is discussed in the following sub-sections.

5.1 Accuracy of Doppler centroid estimation

The accuracy of Doppler centroid estimation depends on the number of processed azimuth lines. Figure 8 shows the accuracy as a function of processed azimuth lines. According to this analysis, 100 lines would be enough to limit the error to be less than 1% of the PRF given the nominal SNR for a nominal ocean sigma0 of 10 dB. For surface water, however, most of the swath can be covered by land, which typically presents lower backscattering coefficients. The number of azimuth lines required to have Doppler centroid estimation accuracy better than 1% for different sigma0 is given in Figure 9. For a sigma0 of -5 dB, it would require about 400 lines for the case of a constant fitting (for comparison, a linear fitting would require 20,000 lines).

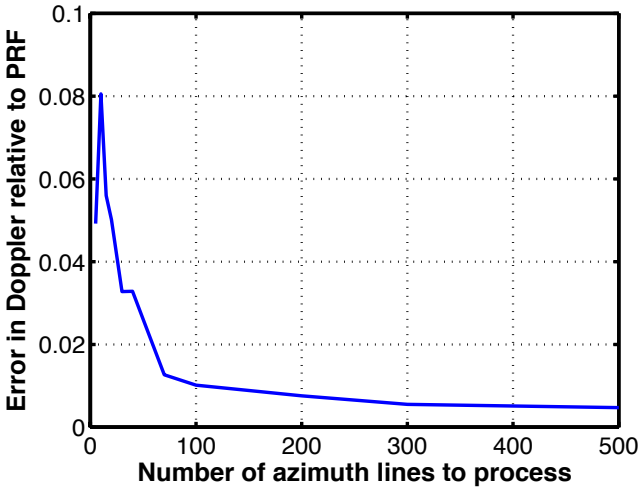

Figure 8: Doppler centroid estimation error (worst case in cross track) as a function of the number of processed azimuth lines with nominal SNR.

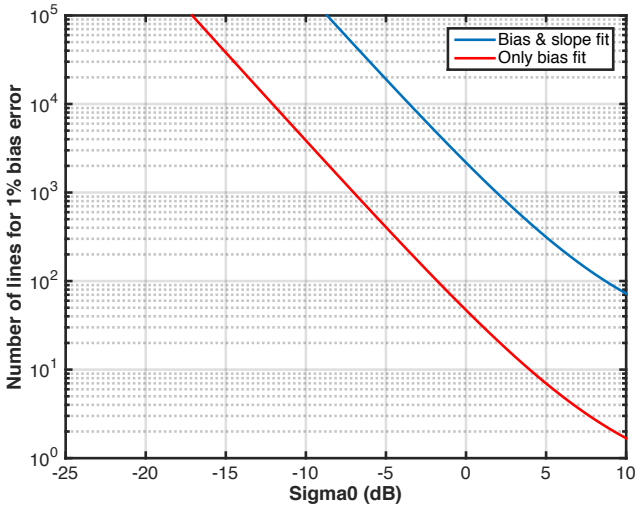

Figure 9: Number of azimuth lines required to have Doppler centroid estimation error 1% vs. sigma0.

Topography and along track sigma0 contrasts can produce fast changes in the Doppler centroid, thereby requiring longer averaging times to meet the accuracy requirement. Rectangular windows are used in the estimation and their lengths in range and azimuth are specified in one of the tables used by FSW. The effects of sigma0 contrast, antenna pattern and motion on the estimation of Doppler centroid have been evaluated, indicating that sharp along track sigma0 contrasts impose the largest error to the Doppler centroid estimates. However, even for a step change in the sigma0 as large as 20 dB, an estimation block of 4,000 range lines would cause a Doppler centroid error of less than 3% (see Figure 10).

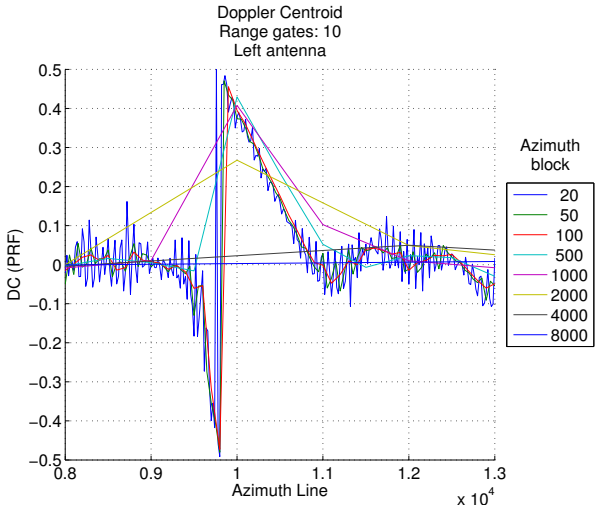

Figure 10: Doppler centroid estimation error for different size of azimuth block averaging with 20 dB along track step contrast.

As discussed in section 4, the Doppler centroid estimation block size or DL_land is restricted to be an integer multiple of the calibration averaging boundary (AV) or 3240 PRIs. The nominal value is 10*AV or 32,400 lines, achieving a Doppler centroid estimation error of less than 1% for sigma0's as low as -15 dB or in areas with large contrasts.

The Doppler centroid estimation takes place before the range filtering and the subsampling of data. There can be some spectral content differences between data used in estimating Doppler centroid and data after filtering, since the transmit/receive bandwidth can go up to 210 MHz (refer to section 4.2) but the filtered data are limited to 200 MHz (the passband of the range filters). The frequency dependence of the antenna pattern in that excess bandwidth could impact the accuracy of the estimated Doppler centroid. Specific analyses conducted to compare the difference in the estimated Doppler centroid with 200 MHz and 210 MHz bandwidth demonstrate that the difference is negligible. Within the allocated transmit bandwidth, we consider the antenna patterns over eleven frequencies from 35.65 GHz to 35.85 GHz in steps of 20 MHz. The Doppler centroids with a single frequency antenna pattern are evaluated for four echo channels. The variation of the Doppler centroid with different frequencies for the left channel of the right swath is given in Figure 11. The other channels have the same level of variations over the frequency band.

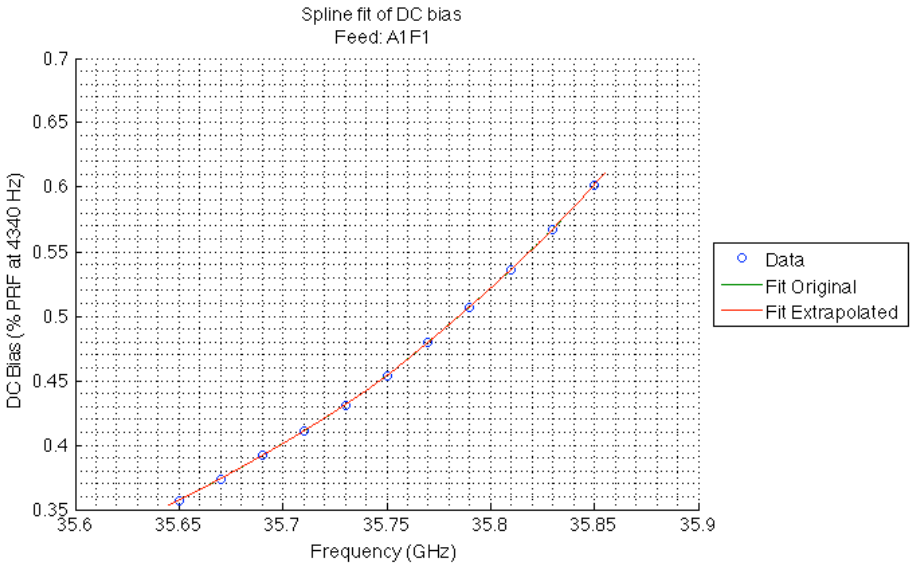

Figure 11: Doppler centroid as a function of the transmit frequency

The eleven data points are spline fitted and extrapolated to generate the variations over frequency bandwidth 210 MHz from 35.645 GHz to 35.855 GHz. The Doppler centroid with a transmit bandwidth is calculated by the equation:

$$DC\_bias_{band} = \frac{1}{2\pi} \measuredangle \left(\overline{\exp\left(\iota\, 2\pi \left(DC\_bias(f)\right)\right)} \right) \tag{2}$$

The cases with the means covered bandwidths 200 MHz and 210 MHz are evaluated and their differences are shown in Table 1. Their difference is less than 0.2%, and it is insignificant.

Channel	Mean DC bias over 200 MHz (%PRF)	Mean DC bias over 200 MHz +/- 5 MHz (%PRF)	Difference (%PRF)
A1F1	0.4630	0.4638	0.00085
A1F2	-0.4214	-0.4222	-0.00076
A2F3	0.4223	0.4231	0.00081
A2F4	-0.4538	-0.4546	-0.00078

Table 1: Difference of Doppler centroid derived from bandwidth 200 MHz and 210 MHz

Within a Doppler centroid estimation block, a PRF change may occur. The PRF could in theory step as fast as every 15 seconds, with a maximum delta of 10 Hz per step. For land processing, the estimation block should therefore have duration less than 15 second; its nominal value is about 6 second. Thus, a PRF change of 10 Hz will only create a Doppler centroid estimation error of 0.23% relative to the

nominal PRF 4420 Hz, if the change is not taken into account. In addition, there is a time difference between Doppler centroid being estimated and applied, and these two events may contain different PRFs. But their time difference should be less than 15 second, and the change of PRF is less than 10 Hz. The Doppler centroid error caused by the change of PRF between estimation and application is less than 0.23%. In the worst case, assuming both PRF change effects occurred, the error is 0.46%. For surface water, the two dominant contributions to the Doppler centroid estimation error (the total error is 7%) are thermal noise of pitch and yaw, and they are 1.54% and 2.3% respectively. The effect of PRF change is insignificant relative to them. Thus, OBP will perform the Doppler removal without correcting for PRF changes.

5.2 Phase variance of filtering and resampling data

The step of filtering and subsampling data will introduce phase error as there can be noise and signal aliasing due to the filter not being perfect. In addition, ripples in its passband can slightly degrade the geometric correlation. These effects are studied and the results are given below.

To achieve high processing speed, the third-band Nyquist filter is selected for this processing step. It is computational efficiency for the SWOT configuration, which requires a downsampling factor of 3. The performance of the third-band Nyquist filter has been analyzed for different filter lengths; taking into consideration the available on-board FPGA resources, a length of 99 coefficients has been chosen. With N = 99, the even filter has length 49, while it is 50 for the odd filter. Some characteristics of this filter are shown below.

The stop-band attenuation and the filter band ripple are shown in Figure 12 and 13 respectively. The stop-band attenuation is 54 dB, and the ripple is 0.02 dB.

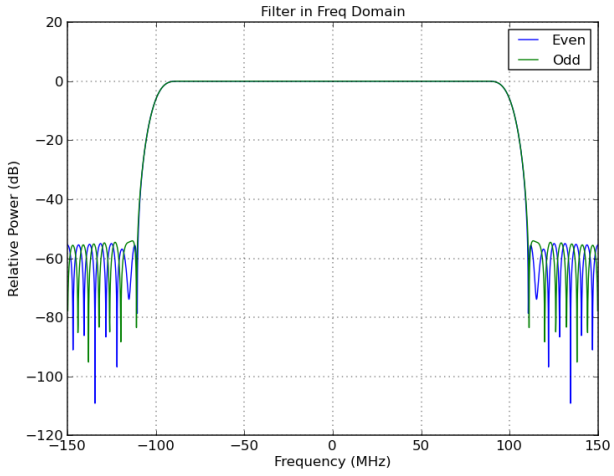

Figure 12: Frequency spectrum of Third-Band Nyquist filter with length 99.

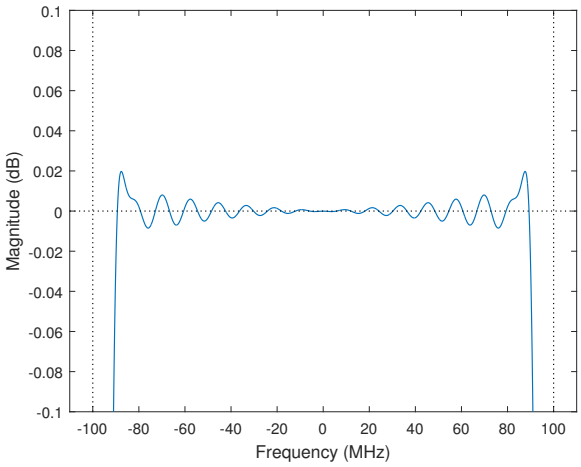

Figure 13: Zoom-in of the pass-band of frequency spectrum of Third-Band Nyquist filter.

For SWOT, height measurements are derived from interferometric phase. To obtain the required high accuracy, the filter should minimize the mean of the phase variance over the required ground range. The equation of phase variance is given by:

$$\langle \Delta\Phi^2 \rangle = \frac{1}{2N_{looks}} \frac{1-\gamma^2}{\gamma^2} \tag{3}$$

where N_{looks} is the product of looks in range dimension and looks in azimuth directions. The number of looks in range direction is determined by the effective bandwidth, the incidence angle at each ground swath distance, and the averaging size. The effective bandwidth is mainly driven by the length of the Third-Band Nyquist filter. Incidence angles are derived from system performance analysis and the averaging size is assumed to be 1 km.

For the purpose of this analysis, the number of looks in azimuth direction is assumed to be constant over ground swath from 10 km to 60 km, and it depends on processing parameters, for example the processing bandwidth.

The correlation γ is the product of noise correlation, geometric correlation and angular correlation. For noise correlation, a constant sigma0 of 10 dB (independent of incidence angle) is assumed and the noise equivalent sigma0 is obtained from system performance analysis; as a result, the thermal SNR can then be evaluated. The overall signal to noise ratio has the additional contributions from the aliasing effect of both noise and signal associated with data subsampling. The definitions of in-band and out-band, and the aliasing effect are shown in Figure 14.

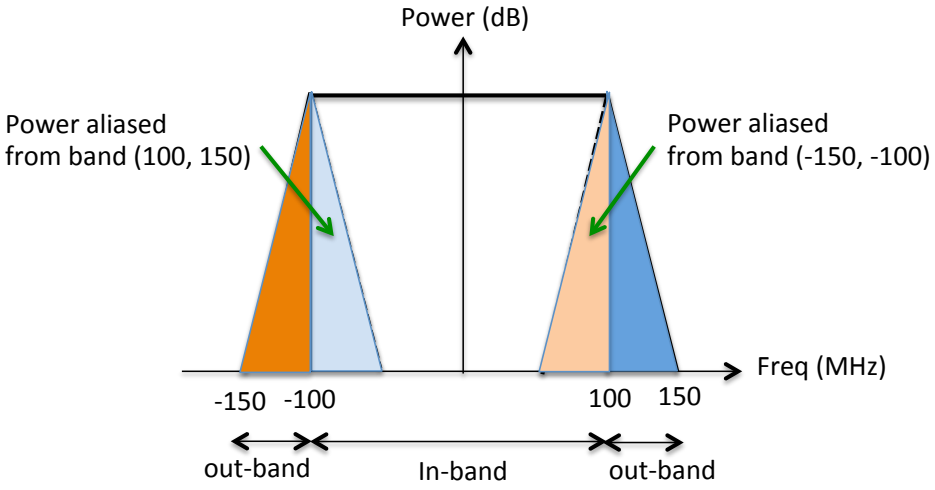

Figure 14: Definitions of in-band and out-band, and the effect of aliasing

Both noise and signal aliasing factors depend on the filter length. Noise aliasing factor is assumed to be the maximum power ratio between in-band and out-band signal, and its nominal value is 54 dB (see Figure 12). Signal aliasing factor is the ratio of power in-band to out-band of the filtered signal, and its nominal value is 23 dB. The noise correlation is dominated by thermal SNR, and its behavior as a function of ground distance is given in Figure 15.

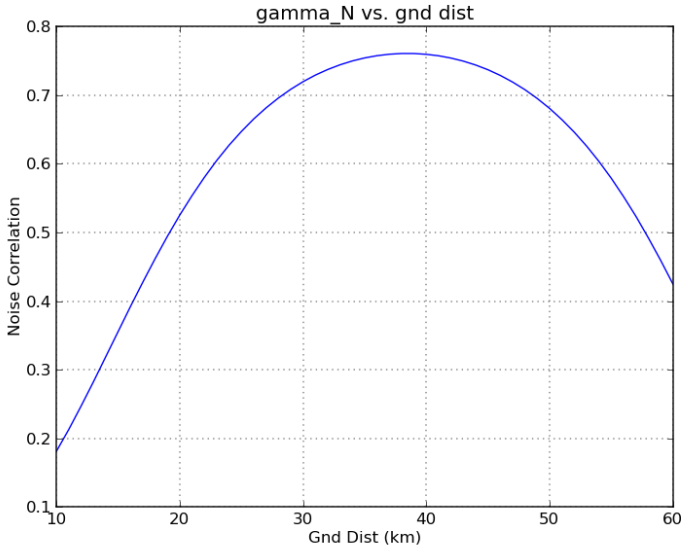

Figure 15: Noise correlation vs. ground distance

Geometric correlation is determined by the equation:

$$\gamma_g = \frac{\int W_1(\omega + w) W_2^*(\omega) d\omega}{\sqrt{\int |W_1(\omega + w)|^2 d\omega \int |W_2(\omega)|^2 d\omega}} \quad (4)$$

W_1 and W_2 are the spectra of the impulse response functions for left and right channels, and the frequency shift ω between the two channels is determined by system performance analysis. In this study, an ideal chirp with bandwidth 210 MHz is considered as the input signal and it goes through the Third-Band Nyquist filter. Then, the output signal is compressed with itself to form the range compressed signal. The compressed signal spectrum for this filter is given in Figure 16. The ripple characteristic is the combined effect of the ripples associated with the filter and the ideal chirp signal. Since the ripple of the filter is 0.02 dB (see Figure 13), the ripple of the compressed signal spectrum is dominated by the nominal amplitude response of an ideal chirp signal.

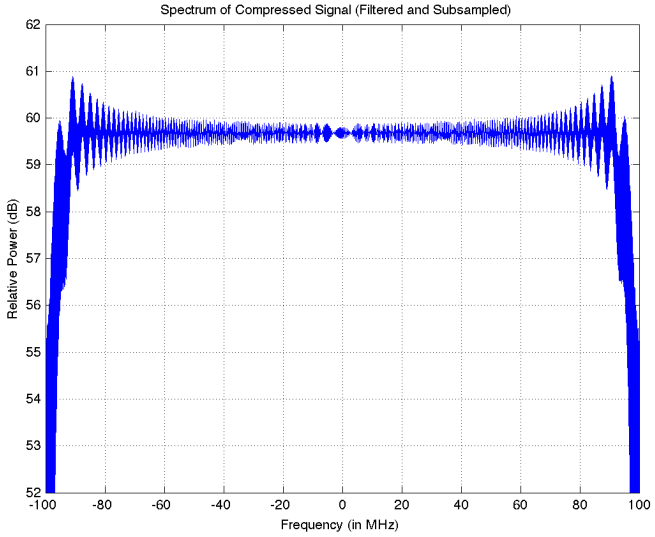

Figure 16: Spectrum of compressed signal (after filtering and subsampling)

With the compressed signal spectrum assigned to both W_1 and W_2, the geometric correlation is evaluated according to Equation 7. Its behavior is shown in Figure 17.

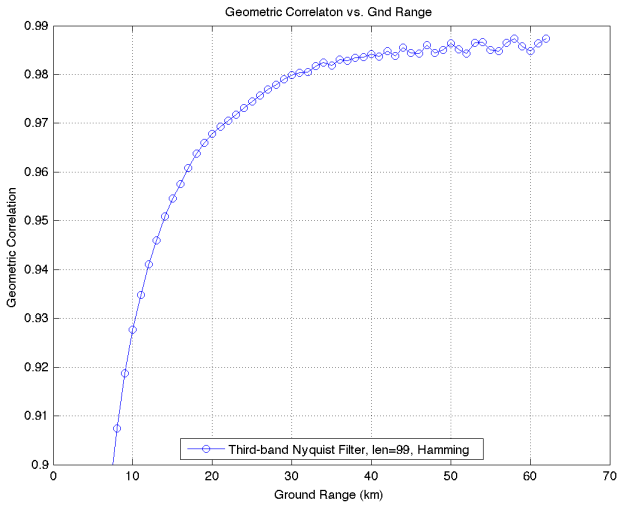

Figure 17: Geometric correlation vs. ground distance

The ripple of the geometric correlation is caused by the ripple of the range compressed signal spectrum. In calculating the geometric correlation, the spectra from the interferometric channels are shifted relative to each other. The frequency shift varies as a function of ground distance, and it can be anticipated that the ripples will go in and out of phase.

Angular correlation is considered to be 1 (i.e., no degradation), as the effect of the antenna dispersion is insignificant for land data. It has been shown the degradation of correlation being negligible in this case (please refer to [3]).

The mean phase variance over ground swath is 0.072/N_az (rad^2) for this filter, where N_az is the number of azimuth looks. The phase variance is not very sensitive to the length of the filter beyond 99, changing by less than 1.4% when the filter length goes from 99 to 199. Taking into account of the factors of resources and processing time, the current filter length 99 is selected.

5.3 Presumming factor

Azimuth presumming of the raw data over land is required to reduce the output data rate and downlink volumes to meet the constraint of the spacecraft. In order to simplify the hardware implementation, the presumming factor is constrained to be an integral multiple of 1/16 (or 0.0625). The current options of this factor are 2.125 and 2.4375. It is a trade between data rate reduction and data accuracy. The baseline value is 2.125. The DWP is adjusted to account for the topography of the scene. The land data have buffers at both ends to allow computation of presummed data when there is a DWP change. Also the DWP will be properly shifted to align the chirp centers of data for presumming if there is a pulse width change.

5.4 BFPQ configuration

To maintain the data rate to within the allocated limit of 349 Mbps for land data processing, azimuth presumming and resampling data to 200 MHz are implemented. The data are then further compressed by Block Floating Point Quantization (BFPQ) technique. This reduces the data from their bitwidth at the output of the presumming block to 3-bits mantissa and 5-bits exponent with block size 32 complex samples. A simulation has been conducted to show that the signal to quantization noise ratio (SQNR) is better than 14 dB for the expected range of sigma0's. With the nominal surface water sigma0 10 dB, the ratio between the quantization and thermal noise is -9 dB. This ratio goes down to -21 dB at the near swath. It shows that SQNR has a negligible impact on SNR.

The simulation for evaluating the BFPQ error involves generating a Gaussian signal, compressing this signal with BFPQ, performing inverse BFPQ, and comparing the difference between input and output signal. In this simulation, the bitwidth of input signal is assumed to be 16-bits. The variance of the Gaussian signal that gives full-scale of 16-bits is one half of square of max amplitude or 87 dB. A sequence of Gaussian signals with 64K samples are generated and their variances are increased from 0 dB to 80 dB with the step size 2 dB. Each signal is quantized with 16-bits integer. This digitized data go through BFPQ with configuration 3-bits mantissa, 5-bits exponent and the block size of 64 real samples (32 complex samples). Then, the BFPQ compressed data are inverse BFPQ'ed. The SQNR is evaluated as the ratio between variance of BFPQ input signal to the variance of difference of BFPQ input signal and inverse BFPQ output signal. The variation of SQNR against the input signal power, which is represented relative to the full-scale power, is shown in Figure 18.

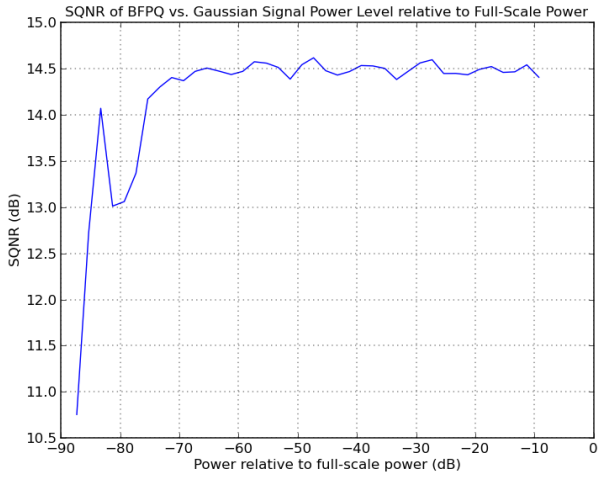

Figure 18: SQNR of BFPQ vs. input signal power level

From Figure 18, it shows that SQNR is greater than 14 dB with the input power level being higher than -75 dB relative to the full-scale power. This simulation assumes the input signal bitwidth to be

16-bits. For bitwidths greater than 16, the change of SQNR is very small for the same input power, and there is no performance impact.

Appendix A. OBP pseudo-code

Golden Model Top Module

Input: rawdataL, rawdataR
Output: fD, BFPQdataL, BFPQdataR

```
1   Estimate Doppler centroid for left channel
            Input: rawdataL
            Output: fDL

2   Estimate Doppler centroid for right channel
            Input: rawdataR
            Output: fDR

3   Compute mean Doppler centroid
            Input: fDL, fDR
            Output:
                  fD = (fDL + fDR)/2

4   Remove Doppler centroid for left channel
            Input: rawdataL, fD
            Output: dopplerremoveddataL

5   Remove Doppler centroid for right channel
            Input: rawdataR, fD
            Output: dopplerremoveddataR

6   Filtering and subsampling for left channel
            Input: dopplerremoveddataL, third-band Nyquist filter
            Output: subsampleddataL

7   Filtering and subsampling for right channel
            Input: dopplerremoveddataR, third-band Nyquist filter
            Output: subsampleddataR

8   Azimuth presumming for left channel
            Input: subsampleddataL, presumming_filter
```

Output: presummeddataL

9 Azimuth presumming for right channel

Input: subsampleddataR, presumming_filter

Output: presummeddataR

10 BFPQ for left channel

Input: presummeddataL, BFPQ tables

Output: BFPQdataL

11 BFPQ for right channel

Input: presummeddataR, BFPQ tables

Output: BFPQdataR

Estimate Doppler centroid

Input: rawdata

Output: fD

1 Calculate pulse pair phase difference in azimuth

2 Average pulse pair phase difference in range and azimuth with averaging windows

3 Compute unwrapped phase

4 Compute constant fit of unwrapped phase

Remove Doppler centroid

Input: rawdata, fD

Output: dopplerremoveddata

1 Receive Doppler centroid correction from FSW, and update Doppler frequency

2 Calculate azimuth phase ramps with fitted Doppler centroid (as a function of ground range) for all range bins

3 Add phases of the last azimuth line of the previous Doppler Centroid estimation block to the phase ramps

4 Apply phase to data

Filter and subsample data in range direction

Input: dopplerremoveddata, third-band Nyquist filter

Output: subsampleddata

1. With specified third-band Nyquist filter length, the filter is generated
2. Run the Doppler removed data through this filter to generate subsampled data

Presum data in azimuth direction

Input: subsampleddata, presumming coefficients

Output: presummeddata

1. Receive the presumming coefficients from FSW
2. Apply the presumming coefficients to data and generate the presummed data

BFPQ rangeline data

Input: presummeddata, BFPQ tables

Output: BFPQdata

1. With specified block size, the standard deviation of the input data in each data block is calculated.
2. The exponent of each block is determined according to the BFPQ table, and also the mantissa of each data in the block.
3. The exponent and mantissa are put together into the output data stream

Appendix B. Summary of Downlinked Data

Calibration frame

The calibration frame rate is 6480 TRI nominally. Some of the essential data for the ground processing include:

1. Ocean Doppler parameters - The six sets of Doppler centroid estimation parameters and the FSW computed Doppler centroid correction.
2. Land Doppler parameters – The six sets of Doppler centroid estimation parameters. The FSW computed Doppler centroid correction and the phases applied to the last azimuth line of a Doppler centroid estimation block.
3. KaRIn Tx LB calibration data – transmit loopback data averaged over AV
4. KaRIn Rx calibration data – receiver calibration data averaged over AV
5. KaRIn HB calibration data – HB calibration data averaged over AV
6. KaRIn Rx only noise data – receiver noise only data averaged over AV

Land frame

The land frame rate depends on presum-factor and PRI, and the time interval between frames is three times the product of presum-factor and PRI (or 3*presume-factor*PRI). The essential data contain:

1. Three sets of land data: each data set include one presummed line from each channel and there are four channels (echoes from left and right antennas for each swath and there are two swaths)
2. Presum-factor and time per land frame

References

[1] Ernesto Rodríguez, “SWOT Project Science Requirements Document”, March 18, 2016, D-61923

[2] R. Kwok and W. T. K. Johnson, “Block Adaptive Quantization of Magellan SAR Data,” *IEEE Transactions on Geoscience and Remote Sensing*, vol. 27, pp. 375–383 (1989).

[3] Eva Peral, “KaRIn: OBP Algorithm Theoretical Basis Document”, November 21, 2014, D-79130